Carbohydrate Research, 160 (1987) 267–281
Elsevier Science Publishers B V., Amsterdam – Printed in The Netherlands

THERMALLY INDUCED CONFORMATIONAL CHANGE OF XANTHAN IN 0.01M AQUEOUS SODIUM CHLORIDE

WEI LIU, TAKAHIRO SATO, TAKASHI NORISUYE, AND HIROSHI FUJITA
Department of Macromolecular Science, Osaka University, Toyonaka, Osaka 560 (Japan)
(Received March 3rd, 1986; accepted for publication in revised form, September 25th, 1986)

ABSTRACT

Light-scattering and viscosity measurements were made on five sonicated samples of sodium xanthan in 0.01M aqueous NaCl at 25 and 80°, temperatures at which the polysaccharide is known to take on certain ordered and disordered conformations, respectively. For two of these samples, measurements were also made at different temperatures between 25 and 80°. From the data obtained for weight-average molecular weight M_w, radius of gyration, and intrinsic viscosity, the following conclusions were derived. (*1*) The ordered conformation of Na xanthan in 0.01M aqueous NaCl at 25° is essentially the same dimerized, double helix as that found previously in 0.1M aqueous NaCl. (*2*) When the temperature is raised from 25 to 80°, the dimer does not dissociate to single chains, but its statistical radius decreases, or remains unchanged, depending on its M_w. (*3*) The disordered conformation at 80° is well represented by a model in which four wormlike chains are joined together by a very short double-helical segment. (*4*) The thermally induced, order–disorder conformational change of xanthan in 0.01M aqueous NaCl is the process of partial melting of the double helix.

INTRODUCTION

Xanthan is an ionic polysaccharide produced by the bacterium *Xanthomonas campestris*. Rees[1,2], Holzwarth[3], and Morris *et al.*[4] concluded from spectroscopic measurements that this polysaccharide in aqueous salt solutions of low ionic strength undergoes an order–disorder conformational change with increasing temperature. Their conclusion has since been confirmed by many workers, using a variety of techniques, such as optical rotation[5–12], circular dichroism[6], potentiometric titration[8], calorimetry[10,13], and viscometry[5,11], but it is still controversial as to what the ordered and disordered conformations imply. The former is likely to be helical dimer according to Paradossi and Brant's[14] and our[15–17] recent findings for a medium of high ionic strength, namely, 0.1M aqueous sodium chloride.

In this work, xanthan in aqueous NaCl of low ionic strength was investigated by light-scattering and viscosity, in order to take a step further into knowledge of

0008-6215/87/$ 03 50 © 1987 Elsevier Science Publishers B V

the order–disorder conformation change. The actual measurements were made at a salt concentration of 0.01M for the reason mentioned in the Experimental section.

EXPERIMENTAL

Samples and solvent. —Five sonicated samples of xanthan, namely, X9-3, X7-3b, X10-4, X13-3-3, and X13-5, were used. The first three were fractions (Na salt) investigated previously[15,16]. The others were newly prepared from Kelco's Keltrol xanthan by extensive sonication, purification, and repeated fractional precipitation, and were then converted into the Na salt form. All the procedures employed in these experiments were essentially the same as those already described[15]; aqueous xanthan solutions of low ionic strength were always kept below 10°.

To suppress complications due to the polyelectrolyte behavior of xanthan, it is advantageous to work with an aqueous salt of higher ionic strength as the solvent. However, according to previous spectroscopic studies[3,6,10], the thermally induced conformational change of xanthan is hardly observable when the salt concentration, C_s, is >0.05M. To find a C_s suitable for observing both ordered and disordered conformations of Na xanthan in an experimentally accessible range of temperature, we measured the specific rotation, $[\alpha]_{300}$, of sample X10-4 in aqueous NaCl at 300-nm wavelength as a function of temperature at several fixed values of C_s.

The unfilled circles in Fig. 1 show the results obtained on successive elevation of temperature, T, with the polymer mass concentrations c at 25° fixed at ~0.5 × 10^{-2} g.cm^{-3} for all the indicated C_s. Except for C_s = 0.1M, the curves fitting these circles for respective C_s rise sigmoidally with increasing T. The sharp rises of $[\alpha]_{300}$

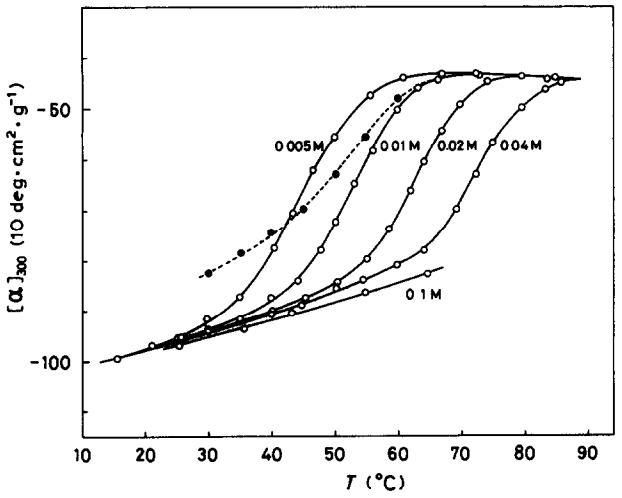

Fig 1 Temperature dependence of $[\alpha]_{300}$ for Na xanthan sample X10-4 in aqueous NaCl of indicated salt concentrations [Key: ○, successive raising of T; ●, successive lowering of T (C_s = 0.01M)]

TABLE I

SPECIFIC REFRACTIVE INDEX INCREMENTS $(\partial n/\partial c)_\mu$ OF Na XANTHAN IN 0 01M AQUEOUS NaCl AT DIFFERENT TEMPERATURES

T (°)	$(\partial n/\partial c)_\mu$	
	at 436 nm	*at 546 nm*
25	0 145	0 142
38	0 143	0 141
50	0 141	0 139
60	0 138	0 136
70	0 133	0 131

confirm previously observed, thermally induced, order–disorder conformational changes[1–12]. Following previous investigators[1–11], we consider that, for a given C_s, the ordered conformation dominates the region of low T in which $[\alpha]_{300}$ stays roughly constant, and the disordered conformation, the region of high T in which $[\alpha]_{300}$ undergoes no more increase. Fig. 1 indicates that the entire change in $[\alpha]_{300}$ from the ordered to disordered conformation is complete in an experimentally accessible T range, i.e., $T <\sim 80°$, only for $C_s \leqslant 0.01$M. Thus, the upper limit of experimentally favorable C_s is 0.01M. However, as already mentioned, use of a lower C_s may introduce complications due to polyelectrolyte effects. For these reasons, we decided to use 0.01M NaCl as the solvent for the present light-scattering and viscosity studies.

The dashed line in Fig. 1 represents the change in $[\alpha]_{300}$ at $C_s = 0.01$M on successive lowering of T. Its difference from the corresponding solid curve indicates that the thermally induced, order–disorder change at $C_s = 0.01$M is irreversible. The irreversibility is diminished at higher C_s, but the data are not shown here. Recently, for a salt-free xanthan solution, Jamieson *et al.*[18] observed a thermal hysteresis very similar to that shown in Fig. 1.

Light scattering and viscometry. — On the basis of Fig. 1, we chose 25 and 80° to investigate the ordered and disordered states of Na xanthan in 0.01M aqueous NaCl by light-scattering and viscosity measurements. Similar experiments were also carried out on two samples, X10-4 and X9-3, between these temperatures. The light-scattering photometer and the viscometers used were the same as those described previously[15–17] (see ref. 15 for details of the experimental procedures).

Increments $(\partial n/\partial c)_\mu$ in specific refractive index for Na xanthan solutions of $C_s = 0.01$M dialyzed at 25, 38, 50, 60, and 70° were determined at the respective temperatures by the method[15] described previously. Here, the subscript μ indicates that the chemical potentials of diffusible components are fixed, while c is varied. The results, presented in Table I, were graphically interpolated, or extrapolated, to estimate $(\partial n/\partial c)_\mu$ at desired T.

Because of the irreversible change in $[\alpha]_{300}$ at 0.01M aqueous NaCl, light-scattering and viscosity data were taken while T was successively elevated; in most

cases, fresh solutions of different polymer concentrations were used at each value of T. At 80°, flow times of solutions for two highest-molecular-weight samples, X7-3b and X9-3, decreased gradually with time. The decrease appeared to continue indefinitely, and its origin was, most likely, degradation of the polymer. However, as far as detected by viscometry, the degradation was so slow that its effects on the data presented here were considered negligible.

RESULTS

Molecular weights and second virial coefficients. — Fig. 2 shows the plots of Kc/R_0 *vs.* c for sample X10-4 in 0.01M aqueous NaCl at 25, 55, and 80°, and also that in 0.1M aqueous NaCl at 25°, in which Na xanthan dissolves as double-helical dimers[15–17]. Here, K is the optical constant, and R_0, the reduced scattering intensity at the zero scattering angle. All the plots have approximately equal intercepts, yielding essentially the same values of M_w (the weight-average molecular weight). Similar results were found for sample X9-3. Thus, it may be concluded that, at least for samples X10-4 and X9-3, Na xanthan in 0.01M aqueous NaCl at T below 80° remains a dimer. In other words, below 80°, the thermally induced, order–disorder conformational change at C_s = 0.01M is an event that occurs in the dimer itself.

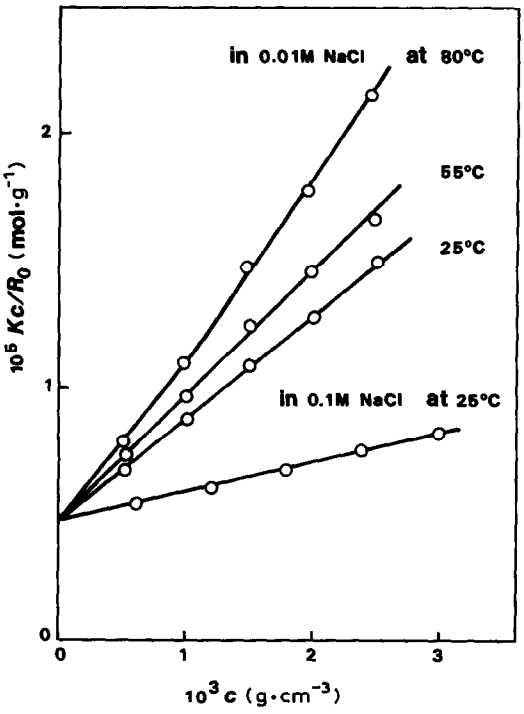

Fig. 2. Plots of Kc/R_0 *vs* c for Na xanthan sample X10-4 in 0 01M aqueous NaCl at 25, 55, and 80°, and in 0 1M aqueous NaCl at 25°

TABLE II

WEIGHT-AVERAGE MOLECULAR WEIGHTS OF Na XANTHAN SAMPLES DETERMINED BY LIGHT-SCATTERING UNDER DIFFERENT SOLVENT CONDITIONS

Sample	$M_w \times 10^{-4}$			
	in 0 01M NaCl		*in 0 1M NaCl* 25°	*in cadoxen* 25°
	25°	80°		
X13-5	5 85	5 85	—	2.9[a]
X13-3-3	10 4	10 4	—	5 3[a]
X10-4	20 6	20 6	20 9	11 0
X7-3b	60 2	60.6	60 3	29 5
X9-3	94 3	92 6	99 4	49 3

[a]Viscosity-average molecular weight

For all samples, the values of M_w determined under different solvent conditions are compared in Table II. Here, the data for solutions in 0.1M aqueous NaCl and cadoxen [tris(ethylenediamine) cadmium dihydroxide] have been taken from our previous papers[15–17]; we note that Na xanthan disperses in the latter solvent as single chains[15]. For every sample, the M_w values in 0.01M aqueous NaCl at 25 and 80° agree with that in 0.1M aqueous NaCl, and are almost twice as large as that in cadoxen. This finding confirms the conclusion that the dimer in 0.01M NaCl does not separate to single chains below 80°. Milas and Rinaudo[6] showed that, below 55°, the M_w of an Na xanthan sample in 0.01M aqueous NaCl remained unchanged with temperature. Although this finding is consistent with ours, these authors took it as evidence for their argument that the thermally induced, order–disorder conformational change in xanthan occurs in a single chain.

The values of A_2 (the second virial coefficient) in 0.01M aqueous NaCl at 25 and 80° are presented in Table III. For all samples studied, A_2 for disordered xanthan dimers at 80° are much larger than those for ordered xanthan dimers at 25°. This is probably due to the fact that electrostatic repulsion is much stronger in the former than in the latter.

Dimensional behavior. — Fig. 3 depicts the angular dependence of particle-scattering function $P(\theta)$ as a function of T for sample X9-3 in 0.01M aqueous NaCl. The values of $\langle S^2 \rangle_z^{1/2}$ (the z-average radius of gyration) obtained are plotted against T in Fig. 4. With increasing T, $\langle S^2 \rangle_z^{1/2}$ sigmoidally decreases in the range of T in which $[\alpha]_{300}$ increases sharply (see Fig. 1 and also Fig. 8 of ref. 12 for sample X9-3). Thus, it may be seen that the thermally induced, order–disorder change of sample X9-3 involves a decrease in its dimensions. However, the $\langle S^2 \rangle_z^{1/2}$ data for a lower-molecular-weight sample (X10-4), also shown in Fig. 4, indicate no change in dimensions with temperature. Hence, we face the problem as to why the temperature dependence of $\langle S^2 \rangle_z^{1/2}$ of the xanthan dimer in 0.01M NaCl is so strongly affected by its M_w.

TABLE III

RESULTS FROM LIGHT-SCATTERING AND VISCOSITY MEASUREMENTS ON Na XANTHAN SAMPLES IN 0 01M AQUEOUS NaCl AT 25 AND 80°

Sample	*25°*					*80°*			
	$M_w \times 10^{-4}$ [a]	$A_2 \times 10^3$ ($cm^3\ mol\ g^{-2}$)	$\langle S^2 \rangle_z^{1/2}$ (*nm*)	$[\eta] \times 10^{-2}$ ($cm^3\ g^{-1}$)	k′	$A_2 \times 10^3$ ($cm^3\ mol\ g^{-2}$)	$\langle S^2 \rangle_z^{1/2}$ (*nm*)	$[\eta] \times 10^{-2}$ ($cm^3.g^{-1}$)	k′
X13-5	5.85	4 56	10 8	0 310	1 52	7 66	12 3	0 396	0 77
X13-3-3	10 4	3 10	17 7	0.750	0.81	5 79	19 3	0.810	0 76
X10-4	20 7	2 02	31 8	1 56	0 75	3.11	32 0	1 58	0 67
X7-3b	60 4	1 75	76 1	5 70	0 43	2 72	60 3	4 25	0 37
X9-3	96	1 26	114	10 0	0 47	1 71	84 0	6 58	0 28

[a] Average of M_w values in 0 01M and 0 1M aqueous NaCl

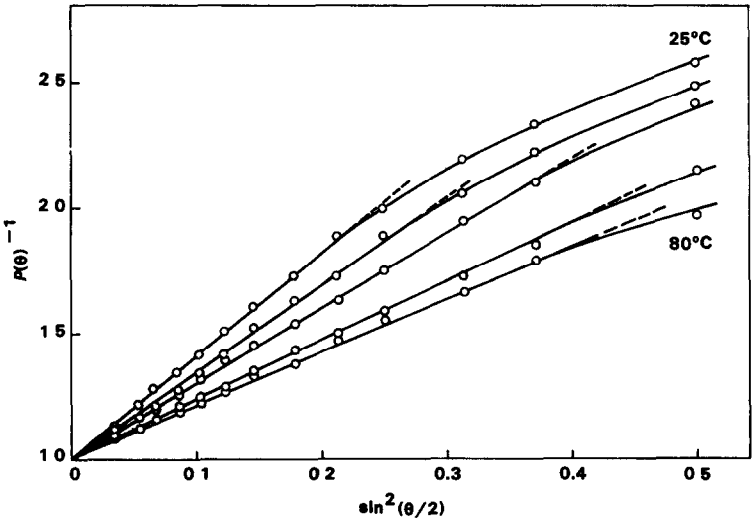

Fig 3 Angular dependence of $P(\theta)^{-1}$ for Na xanthan sample X9-3 in 0 01M aqueous NaCl at 25, 50, 60, 70, and 80° (from top to bottom); wavelength, 546 nm

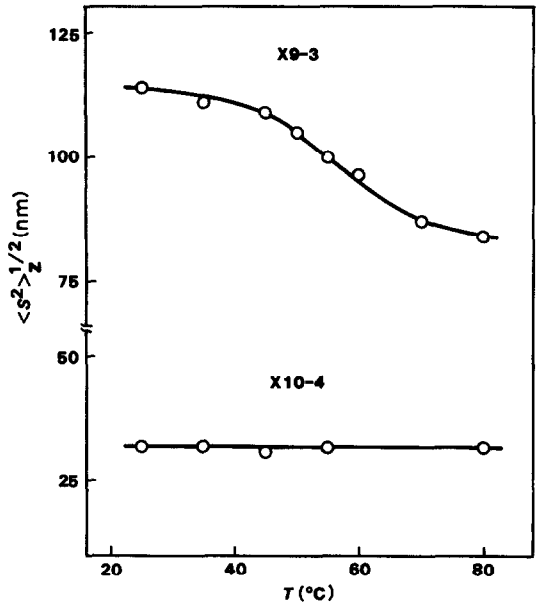

Fig 4. Temperature dependence of $\langle S^2 \rangle_z^{1/2}$ for Na xanthan samples X9-3 and X10-4 in 0 01M aqueous NaCl

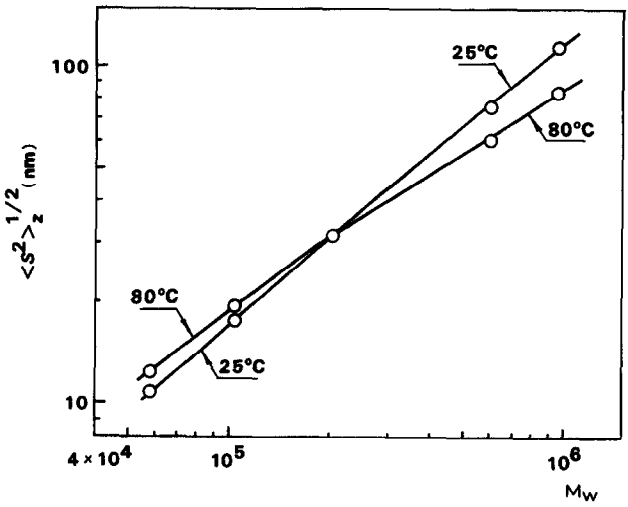

Fig 5 Molecular-weight dependence of $\langle S^2\rangle_z^{1/2}$ for Na xanthan in 0 01M aqueous NaCl at 25 and 80°

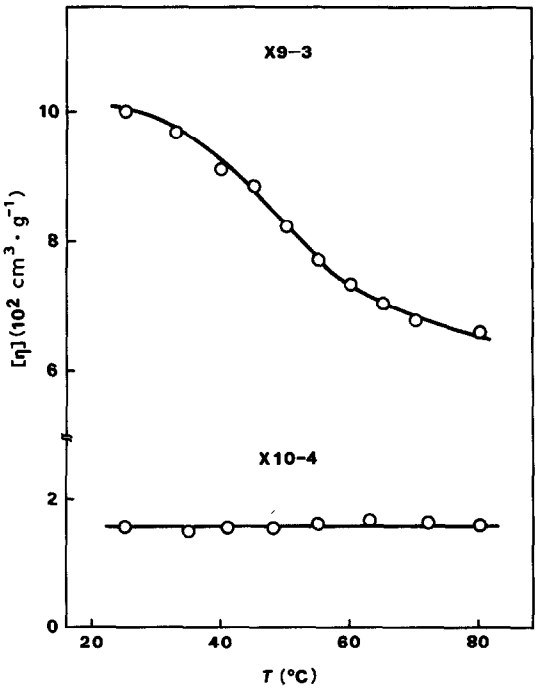

Fig 6 Temperature dependence of $[\eta]$ for Na xanthan samples X9-3 and X10-4 in 0 01M aqueous NaCl

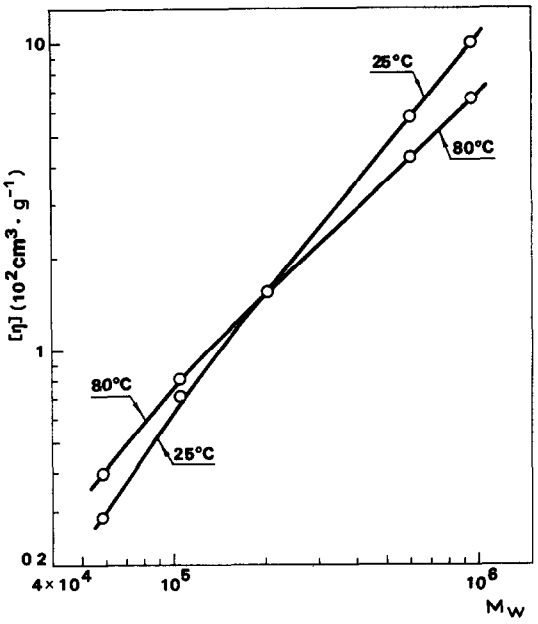

Fig 7 Molecular-weight dependence of $[\eta]$ for Na xanthan in 0.01M aqueous NaCl at 25 and 80°

The values of $\langle S^2\rangle_z^{1/2}$ in 0.01M aqueous NaCl at 25 and 80° are presented in the fourth and eighth columns of Table III, and their molecular-weight dependence is illustrated in Fig. 5. It is striking that the curves at these two values of T intersect at an M_w of $\sim 2 \times 10^5$, indicating that, for M_w below the intersection, the disordered xanthan at 80° has a larger statistical radius than the ordered xanthan at 25°. The slope of the curve at 80° is ~0.68, which suggests that the overall conformation of the disordered xanthan dimer can be delineated as an expanded, random coil. On the other hand, the slope at 25° is ~0.9 below $M_w \sim 2 \times 10^5$, indicating that ordered xanthan dimers of low molecular weights are rodlike.

Viscosity behavior. — Fig. 6 shows the temperature-dependence of $[\eta]$ for samples X9-3 and X10-4 in 0.01M aqueous NaCl. With increasing T, $[\eta]$ for the former decreases sigmoidally, while that for the latter stays almost constant. These features are comparable to those of $\langle S^2\rangle_z^{1/2}$ shown in Fig. 4.

The values of $[\eta]$ and Huggins' constant k' in 0.01M aqueous NaCl at 25 and 80° are given in Table III, and these $[\eta]$ values are plotted double-logarithmically against M_w in Fig. 7. The two curves intersect at $M_w \sim 2 \times 10^5$. This is consistent with the finding in Fig. 5 that, for $M_w < 2 \times 10^5$, the statistical radius of the disordered xanthan is larger than that of the ordered xanthan. For $M_w > 2 \times 10^5$, the slope of the viscosity curve at 80° is ~0.9, which is very close to 0.92 determined by Brown *et al.*[19] for Na *O*-(carboxymethyl)cellulose (CMC), a single coil expanded by electrostatic repulsion, in 0.01M aqueous NaCl. This agreement substantiates the concept of the expanded-coil conformation of the disordered xanthan suggested from the $\langle S^2\rangle_z^{1/2}$ data.

The slope of the viscosity curve for the ordered xanthan gradually decreases from 1.5 to 1.2 with increasing M_w. This decrease suggests an unperturbed, wormlike chain to be a relevant model for the ordered xanthan, as was the case[15–17] for the double helix in 0.1M aqueous NaCl at 25°.

DISCUSSION

Ordered conformation. — The solid curve of $[\alpha]_{300}$ *vs.* T for C_s = 0.01M in Fig. 1 almost merges with that for C_s = 0.1M below 30°. If the measured $[\alpha]_{300}$ reflects the overall conformation, or structure, of Na xanthan, it is possible to conclude from this that the ordered dimer of Na xanthan in 0.01M aqueous NaCl at 25° assumes the same double-helical conformation as that in 0.1M aqueous NaCl at 25°. The following comparisons may strengthen the conclusion.

In Fig. 8, our $\langle S^2\rangle_z^{1/2}$ and $[\eta]$ data for the ordered xanthan in 0.01M aqueous NaCl are compared with the previous data[15–17] for the double helix in 0.1M aqueous NaCl at the same temperature, with unpublished data added (see the legend to Fig. 8). Here, the curves represent the theoretical values calculated for the xanthan

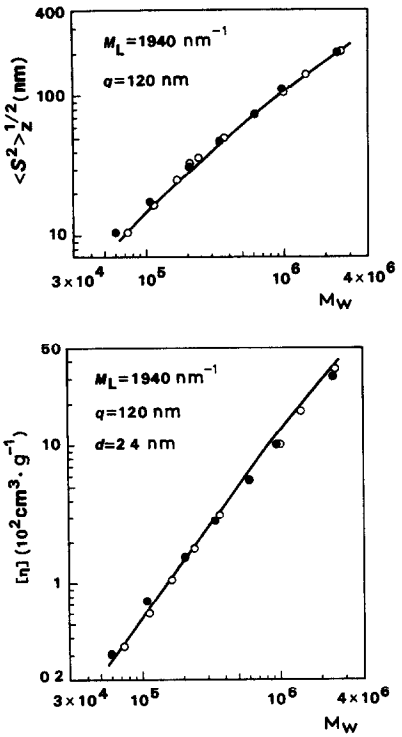

Fig 8 Statistical radii and intrinsic viscosities of Na xanthan samples in 0.01M aqueous NaCl at 25° (●), compared with those[15–17] in 0 1M aqueous NaCl at 25° (○), and calculated values (the solid lines) for the double helix of Na xanthan (see the text for the indicated parameter values). Filled circles at M_w = 34 0 × 10^4 and 248 × 10^4, unpublished data.

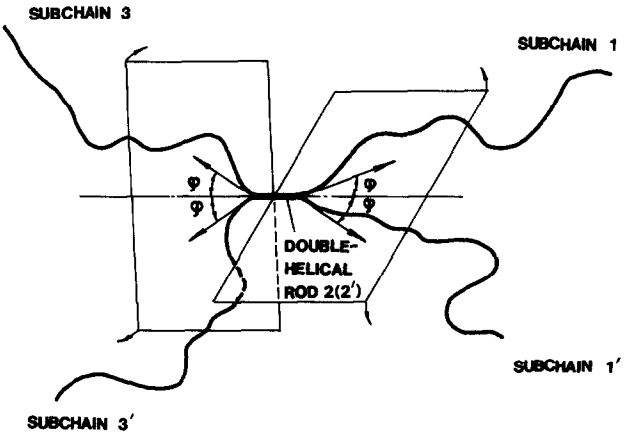

Fig 9 Wormlike dimer model for the xanthan dimer in 0 01M aqueous NaCl at 80°

double-helix by use of Benoit and Dotsy's theory[20] of $\langle S^2 \rangle$ and the theory of Yamakawa *et al.* for evaluating $[\eta]$ for unperturbed wormlike chains with M_L (the molar mass per unit contour length) = 1940 nm^{-1}, q (the persistence length) = 120 nm, and d (the helix diameter) = 2.4 nm; these values were taken from our previous analysis[17], which showed that the double helix in 0.1M aqueous NaCl at 25° is characterized by M_L = 1940 ±100 nm^{-1}, q = 120 ±20 nm, and d = 2.4 ±0.3 nm, and that the M_L value of 1940 nm^{-1} corresponds to a helix pitch of 0.47 nm per main chain residue. The data points for $\langle S^2 \rangle_z$ and $[\eta]$ in 0.01M aqueous NaCl come quite close to those in 0.1M aqueous NaCl, and fit to the respective, theoretical curves. We take this agreement as supporting the aforementioned conclusion.

Disordered conformation. — Our data for $\langle S^2 \rangle_z$ and $[\eta]$ support the suggestion that the xanthan dimer in 0.01M aqueous NaCl at 80° behaves as an expanded, random coil, and also reveal the striking feature that the statistical radius of this dimer is larger than that of the rodlike, double helix with the same M_w if M_w is $<2 \times 10^5$. The following is an attempt to explain the latter by means of a plausible molecular model.

1. Model and assumptions. — According to our previous analysis[12] of optical rotatory dispersion data, the local conformation of the disordered xanthan in 0.01M aqueous NaCl at 80°, reflected by $[\alpha]_{300}$, is similar to that of a single xanthan random-coil[15] in cadoxen. If this fact is combined with the present observation that $[\alpha]_{300}$ in the same aqueous salt remained constant at T above ~80° (see Fig. 1), it may be considered that the disordered xanthan at 80° is a randomly coiled dimer containing only a small number of double-helical residues.

Therefore, we replaced this dimer by the model* shown in Fig. 9, which

*The model assumes that the disordered xanthan dimer contains no loop. This assumption was suggested by the fact[23] that the melting behavior of short, DNA double-helices (M_w <10^6) can be well described by a model in which no loop formation is allowed.

consists of four extended-coil subchains 1, 1′, 3, and 3′ (1 = 1′, and 3 = 3′) joined by a very short, double-helical rod 2. Theoretically, the double-helical section can appear at any portion of the dimer with equal probability[24]. This condition is taken into account in the subsequent analysis.

We modeled each of the four extended-coil subchains by an unperturbed, wormlike chain on the basis of Tricot's analysis[25], which showed that the molecular-weight dependence of $[\eta]$ for several polyelectrolytes in aqueous salt of C_s ranging from 0.003 to 5M can be described by the theory of Yamakawa *et al.*[21,22] for unperturbed, wormlike chains. We ignored inter-subchain repulsions, except those very near the helix ends, which are estimated on the following assumptions. (*1*) The initial tangent vectors (the arrows in Fig. 9) of either pair of wormlike subchains (1 and 1′, or 3 and 3′) are coplanar to the helix, and each makes a supplementary angle of φ with the helix, and (*2*) the two pairs of tangent vectors can rotate about the helix axis independently, as schematically shown in Fig. 9 by two rotating planes which include the rod in common.

2. Analysis. — We calculated $\langle S^2 \rangle$ for the foregoing dimer model and obtained*

$$\frac{\langle S^2 \rangle}{4q_s^2} = \frac{L}{4} - \frac{3}{8} + \frac{3}{8L} - \frac{3}{16L^2}(1 - e^{-2L}) + \gamma \left[-\frac{1}{24} + \frac{5}{16L^2} - \frac{3}{16L^2}\left(1 + \frac{2}{3L}\right)(1 - e^{-2L}) - \frac{1}{64L^3}(1 - e^{-4L}) \right] \tag{1}$$

with

$$L = \frac{(M/2)}{2q_s M_{L,s}} \tag{2}$$

and

$$\gamma = \cos 2\varphi. \tag{3}$$

Here, q_s and $M_{L,s}$ are the persistence length and molar mass per unit contour length of each wormlike subchain, respectively, and M, the molecular weight of the dimer. Because the double-helical rod was assumed to be very short compared with the total contour length of each single chain, Eq. *1* contains no parameter other than q_s, $M_{L,s}$, and γ, which are associated with the wormlike subchains. Although, as

*The calculation was performed first on four freely rotating chains joined by a short rod, and then the resulting expression of the radius of gyration was converted into that for our wormlike, dimer model by taking a continuous limit, *i e* , by the standard method[26] for deriving the mean-square dimensions of a wormlike chain

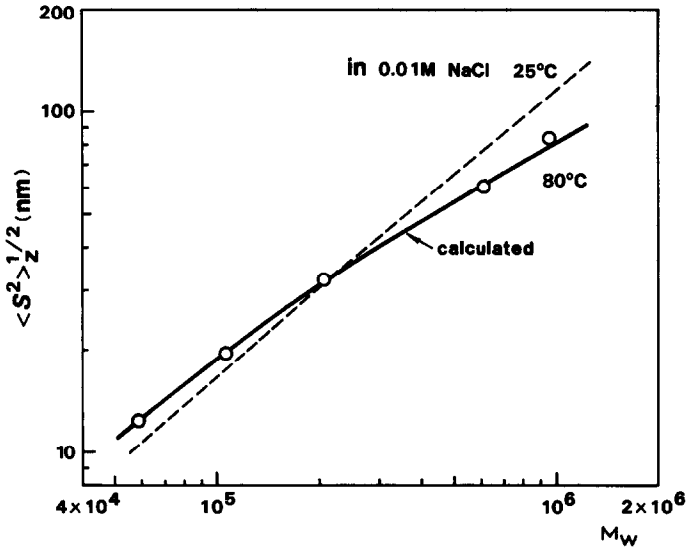

Fig 10 Comparison between the measured $\langle S^2 \rangle_z^{1/2}$ for the xanthan dimer in 0 01M aqueous NaCl at 80° and the values (the solid line) for the wormlike dimer model calculated from Eq *1* with $\gamma = -2/3$, $M_{L,s} = 750$ nm^{-1}, and $q_s = 21$ nm [The dashed line represents the $\langle S^2 \rangle_z^{1/2}$ data in 0 01M aqueous NaCl at 25° reproduced from Fig 5]

will be shown, $\langle S^2 \rangle$ is insensitive to γ, we proceeded with γ taken to be $-2/3$, a value close to the -0.62 given by the bond angle 116° for the (1→4)-β-glucosidic oxygen atom[27].

If L >3, Eq. *1* with Eq. *2* and $\gamma = -2/3$ gives an asymptotic form as

$$(M/\langle S^2 \rangle)^{1/2} = 2(M_{L,s}/q_s)^{1/2} + 50 M_{L,s}^{3/2} q_s^{1/2}/9M + O(M^{-2}),$$

which indicates that $(M_{L,s}/q_s)^{1/2}$ and $M_{L,s}^{3/2} q_s^{1/2}$ can be estimated from the intercept and initial slope of a plot of $(M/\langle S^2 \rangle)^{1/2}$ *vs.* $1/M$. However, the evaluation of $M_{L,s}^{3/2} q_s^{1/2}$ is feasible only when accurate $\langle S^2 \rangle$ data are available for many high-molecular-weight samples. Therefore, we first evaluated the ratio $M_{L,s}/q_s$ from the intercept of $(M_w/\langle S^2 \rangle_z)^{1/2}$ plotted against $1/M_w$, and then searched for a set of q_s and $M_{L,s}$ leading to close agreement between our $\langle S^2 \rangle_z$ data and Eq. *1* with $\gamma = -2/3$ and the known value of $M_{L,s}/q_s$.

In this way, we obtained 750 ±100 nm^{-1} for $M_{L,s}$ and 21 ±3 nm for q_s. The former may be compared with the $M_{L,s}$ value of 840 nm^{-1} evaluated with the virtual bond-length of 0.547 nm for β-(1→4)-D-glucose[27] and the molar mass of 460 per main chain residue of our Na xanthan[15,17]. The latter is also close to the persistence length of 18 nm estimated by Tricot[25] for Na CMC in 0.01M aqueous NaCl from the $[\eta]$ data of Brown *et al.*[19]. However, these q_s values do not always reflect the chain stiffness, as they may involve excluded-volume effects.

The solid line in Fig 10 confirms the foregoing finding that the disordered

xanthan in 0.01M aqueous NaCl at 80° is characterized with $\gamma = -2/3$, $M_{L,s} = 750$ nm^{-1}, and $q_s = 21$ nm. The dashed line represents the $\langle S^2 \rangle_z^{1/2}$ data for the ordered xanthan dimer, *i.e.*, the double helix, in 0.01M aqueous NaCl at 25°, reproduced from Fig. 7. Thus, we find that, in the range of M_w studied, our wormlike chain-model can quantitatively describe the statistical radius of the disordered xanthan at 80° and also predicts it to be larger than that of the rodlike, ordered xanthan for $M_w < 2 \times 10^5$. Qualitatively, the latter may be explained as follows.

At a high M, each monomer chain in the disordered dimer, being randomly coiled, has a statistical radius $\langle S^2 \rangle_1^{1/2}$, much smaller than that of the rodlike monomer chain in the ordered dimer, but the difference becomes smaller as M is lowered. Because $\langle S^2 \rangle^{1/2}$ of the disordered dimer contains additional contributions from the distances between different subchains ($1 - 1'$ and $3 - 3'$ in Fig. 9), it becomes larger than $\langle S^2 \rangle^{1/2}$ of the ordered dimer when M is lowered below a certain value at which these contributions exceed the difference in $\langle S^2 \rangle_1^{1/2}$

It is interesting to consider a limiting case, $\varphi = 0$, for which our dimer model reduces to two wormlike chains contacting themselves tangentially at a single contour point. In this case, $\gamma = 1$, and the data points in Fig. 10 can be fitted equally well by Eq. *1* with $M_{L,s} = 650$ nm^{-1} and $q_s = 18$ nm (compare these with $M_{L,s} = 750$ nm^{-1} and $q_s = 21$ nm for $\gamma = -2/3$). Thus, we find that the characteristic, dimensional behavior of the disordered xanthan dimer is insensitive to the angle φ.

ACKNOWLEDGMENTS

We thank Miss H. Kitagawa for her help in optical rotation and viscosity measurements. W Liu expresses his appreciation to the Ministry of Education, the People's Republic of China, which allowed him to study at the graduate school of Macromolecular Science, Faculty of Science, Osaka University. This work was supported, in part, by the Institute of Polymer Research, Osaka University.

REFERENCES

1 D A REES, *Biochem J*, 126 (1972) 257–273
2 D A REES, *Pure Appl Chem*, 53 (1981) 1–14
3 G HOLZWARTH, *Biochemistry*, 15 (1976) 4333–4339
4 E R MORRIS, D A REES, G YOUNG, M D WALKINSHAW, AND A DARKE, *J Mol Biol*, 110 (1977) 1–16
5 I C M DEA, E R. MORRIS, D A REES, E J WELSH, H A BARNES, AND J PRICE, *Carbohydr Res*, 57 (1977) 249–272
6 M MILAS AND M. RINAUDO, *Carbohydr Res*, 76 (1979) 189–196
7 I T NORTON, D M GOODALL., E R MORRIS, AND D A REES, *J Chem Soc Chem Commun*, (1980) 545–547
8 M. MILAS AND M RINAUDO, *Solution Properties of Polysaccharides, ACS Symp Ser*, 150 (1981) 25–30
9 S A FRANGOU, E R MORRIS, D A REES, R K RICHARDSON, AND S B ROSS-MURPHY, *J Polym Sci, Polym Lett Ed*, 20 (1982) 531–538
10 I T NORTON, D. M GOODALL, S A FRANGOU, E R MORRIS, AND D A REES, *J Mol Biol*, 175 (1984) 371–394

11 M. MILAS AND M. RINAUDO, *Polym. Bull.*, 12 (1984) 507–514, M MILAS, M. RINAUDO, AND B. TINLAND, in G O PHILLIPS, D. J. WEDLOCK, AND P. A WILLIAMS (Eds), *Gums and Stabilisers for the Food Industry 3,* Elsevier Appl. Sci., London & New York, 1985, pp. 637–644.
12 H KITAGAWA, T. SATO, T. NORISUYE, AND H FUJITA, *Carbohydr Polym* , 5 (1985) 407–422
13 S PAOLETTI, A. CESARO, AND F. DELBEN, *Carbohydr. Res.*, 123 (1983) 173–178
14 G. PARADOSSI AND D. A. BRANT, *Macromolecules,* 15 (1982) 874–879.
15 T. SATO, T. NORISUYE, AND H FUJITA, *Polym. J.*, 16 (1984) 341–350.
16 T. SATO, S. KOJIMA, T. NORISUYE, AND H. FUJITA, *Polym J.*, 16 (1984) 423–429.
17 T SATO, T. NORISUYE, AND H. FUJITA, *Macromolecules,* 17 (1984) 2696–2700
18 A M JAMIESON, J. G. SOUTHWICK, AND J BLACKWELL, *Faraday Symp. Chem. Soc.*, 18 (1983) 131–143.
19 W BROWN, D. HENLEY, AND J. OHMAN, *Ark Kemi,* 22 (1964) 189–205
20 H. BENOIT AND P. DOTY, *J. Phys Chem.*, 57 (1953) 958–963.
21 H. YAMAKAWA AND M. FUJII, *Macromolecules,* 7 (1974) 128–135.
22 H YAMAKAWA AND T. YOSHIZAKI, *Macromolecules,* 13 (1980) 633–643.
23 D M CROTHERS, N. R. KALLENBACH, AND B H ZIMM, *J Mol Biol.*, 11 (1965) 802–820.
24 See, for example, D POLAND AND H. A. SCHERAGA, *Theory of Helix–Coil Transition in Biopolymers,* Academic Press, New York and London, 1970
25 M TRICOT, *Macromolecules,* 17 (1984) 1698–1704
26 H YAMAKAWA, *Modern Theory of Polymer Solutions,* Harper & Row, New York, 1971.
27 See, for example, K. D. GOEBEL, C. E. HARVIE, AND D. A. BRANT, *Appl. Polym. Symp.*, 28 (1976) 671–691.